Diyala Journal of Engineering Sciences

Journal homepage: https://djes.info/index.php/djes

ISSN: 1999-8716 (Print); 2616-6909 (Online)

Synthesis and Diagnosis of New Heterocyclic Compound as Corrosion Inhibitor for Mild Steel in Acidic Solution

Hussein S. Hassan[1], Khalid H. Rashid[1], Khalida F. AL-Azawi[2], Anees A. Khadom[3*], and Hameed B. Mahood[4]

[1] Department of Chemical Engineering, University of Technology, Iraq, Baghdad, 10066 Iraq
[2] Applied Chemistry Division, Applied Science Department, University of Technology, 10066 Iraq
[3] Department of Chemical Engineering, University of Diyala, Baquba, 32001 Iraq
[4]Centre for Sustainable Cooling, School of Chemical Engineering, University of Birmingham, Birmingham City, UK.

ARTICLE INFO

Article history:
Received February 24, 2024
Revised October 2, 2024
Accepted October 7, 2024
Available online December 1, 2024

Keywords:
Steel
Synthesis
Corrosion
Inhibitor
DFT
SEM

ABSTRACT

The detrimental impact of corrosion on industrial metals, especially mild steel under acidic conditions, underscores the need for the development of effective corrosion inhibitors. In the present work, a new anticorrosion chemical named 2-(2-anthracen-9-yl)-3-chloro-4-oxoazetidin-1-y1)-1- methyl-1H-imidazol-4(5H)-one (AOMI) was synthesized, identified, and assessed for the protection of low-carbon steel corrosion in one molar hydrochloric acid solution. Experimental procedures included weight loss, electrochemical, surface morphological, FTIR, 1H NMR, and hardness measurements, while computational analyses involved quantum chemical calculations. The investigation revealed that AOMI significantly reduced corrosion rates with maximum inhibition efficiencies of 90% at 80 ppm and 60 ºC. A spontaneous monolayer was formed on the metal surface. The adsorption of this layer was according to the Langmuir isotherm. SEM and AFM images showed the presence of the protective layer. The experimental results were validated by computational simulations, which showed that bonds were formed with the mild steel surface.

1. Introduction

In the oil and gas sector, acidizing oil wells is a common procedure that is often used during drilling and pipeline and equipment transportation [1]. Mineral acids, such as hydrochloric acid and sulfuric acid, are usually used in this procedure at concentrations between 15 to 28% [2]. Because carbon steel alloys are inexpensive, mechanically strong, ductile, and hardenable, they are widely used in industrial applications [3]. On the other hand, the use of aggressive solution, such as acids may cause damages to the steel surfaces [4]. Effective corrosion protection systems have been the focus of a concentrated effort to solve this expensive and unwanted phenomenon. Conventional methods, such cathodic protection and protective coatings, have been studied but are occasionally limited by their high labour and cost associated with them [5]. Considering these issues, the development of a new, eco-friendly organic compound as a corrosion inhibitor is a potential workaround. By creating protective barriers on steel surfaces, this technique has been effective in prolonging the life of the metals. Strong interaction with the iron atoms is made possible by the unique structures of the

* Corresponding author.
E-mail address: aneesdr@gmail.com
DOI: 10.24237/djes.2024.17411

This work is licensed under a Creative Commons Attribution 4.0 International License.

organic molecules (presence of heteroatoms) [6, 7].

According to the literature, the use of heterocyclic organic corrosion inhibitors was a significant was for corrosion control. The action of heterocyclic compounds can be achieved through adsorption on metal surfaces, which isolates the latter from the corrosive solution [8, 9, 10]. Several factors may affect the adsorption process, such as the corrosion inhibitor nature, metal nature, and surrounding conditions [11]. One can find inhibitors from a number of sources, such as chemical providers, expired pharmaceuticals, natural plant extracts, etc. Synthesized organic molecules represent one of the most significant, effective, and straightforward sources [12]. The majority of organic chemicals with multiple bonds, oxygen, sulfur, nitrogen, and phosphorus had strong inhibitory effects. The bulk of potent inhibitors, as per the literature, are heterocycles featuring unsaturated (double and triple) bonds and functional groups [14]. In general, heteroatoms' electron-rich cores actively engage in the binding process with the metallic surface. Imidazole and its derivatives have recently received an attention due to low cost, solubility in water, and ease of synthesis.

The aim of the current work is to synthesis a new imidazole derivative, which can be used as a corrosion inhibitor for low-carbon steel in a hydrochloric acid solution. The effectiveness of 2-(2-anthracen-9-yl)-3-chloro-4-oxoazetidin-1-y1)-1-methyl-1H-imidazol-4(5H)-one (AOMI) was examined through both theoretical and experimental investigations.

2. Experimental work

2.1 Synthesis of the inhibitor

A full procedure for the synthesis process was given in details in our previous work with some exception in the raw materials [13]. $C_{21}H_{16}N_3O_2Cl$ was the chemical formula of AOMI (molecular weight was 377 g/mol, 80% yield, 224–226 ºC melting point (measured by capillary method), and yellow color. Figure 1, shows a schematic diagram of the synthesis process.

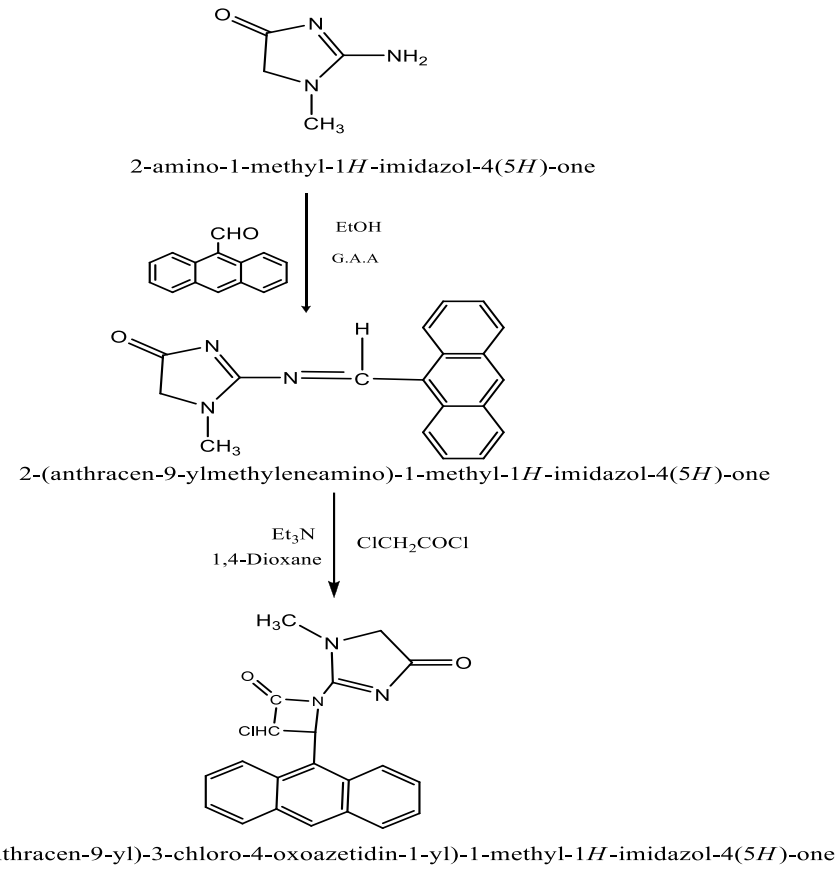

Figure 1. Scheme of the synthesis process of AOMI

2.2 Mass loss and electrochemical tests

ASTM 283/C mild steel was used as samples. It has the following chemical compositions (wt.%): 0.11 C, 0.32 Mn, 0.06Al, 0.029 Si, 0.05 Cu, and Fe is the balance. A concentrated hydrochloric acid (32%) was used to prepare 1M acid, which is used as a corrosive solution. The mass loss, open circuit potential (OCP), potentiodynamic polarization (PDP), and electrochemical impedance spectroscopy (EIS) were the main corrosion measurements. They used to determine the corrosion rates and other electrochemical parameters. In the mass loss (sometimes called weight loss) technique, ASTM 283/C mild steel samples were cut in the dimensions (in centimeters) of 3×1×0.1 to give an average surface area of 6.8 cm^2. To get a smooth surface, ASTM 283/C mild steel samples were cleaned and prepared as mentioned in our previous work [13]. In addition, all setting of apparatuses, such as a scan rate (1 mV/sec) and the scan range (-250 to +250 mV) of PDP method, and the frequency range (100 kHz to 10 mHz with a perturbation amplitude of 10 mV at stable OCP) for EIS were also given in details in our previous work [13]. Z-View software was then utilized to assess the EIS data using an equivalent electrical circuit model.

2.3 Surface and corrosive solution tests

The surface testes were for polished, uninhibited solution, and inhibited with 80 ppm of AOMI (at 60 ^oC). The tests included, x-ray diffraction (XRD), atomic force microscopy (AFM), scanning electron microscopy (SEM). In addition, the film thickness and roughness tests were conducted using a coating thickness meter (MCTM) (REED Instruments Analytial-China) and the surface roughness was evaluated using the Hobson-Taysurf device (UK). The hardness test were subjected to the Vickers microhardness apparatus using the optical microscopy (LARYEE equipment, Germany). The highest load is 9.8 Newtons, the magnification was 100X, the indentation length was measured as the mean of two readings, and the maximum load was maintained for 20 seconds per reading. The hardness of the metal surface was measured at three conditions: before immersion, after immersion for three hours in an uninhibited corrosive solution, and after dipping for three hours in the presence of 80 ppm of AOMI.

For the structure of inhibitor and solution tests, FTIR, ^{1}HNMR, and UV-vis spectra were achieved.

3. Results and discussion

3.1 Characterization of AOMI

FTIR spectrum of AMOI was shown in Figure 2A. The stretching vibration bands that correspond to 3440, 2930, 1688, 1686,1650, 1611, and 1551 1/cm. This may be due to OH bond, CH in aromatic, CO double bond in cyclic amide, CN double bond, and CC double bond in the aromatic, respectively [15]. The ^{1}HNMR spectra of AOMI (Figure 2B) showed signals at δ (1.16, 2.88) ppm of (t,6H, $2OCH_3$) ;δ (2.39, 2.62) ppm of (s,3H, $N\text{-}CH_3$); δ (2.95, 3.36) ppm of (s, 2H, CH_2-C=O), δ (6.67-8.26) ppm of (m,2H, aromatic ring) and δ (4.10) ppm of (s,1H, OH) [16]. In addition, there is a signal at δ (2.52) ppm due to the solvent [13].

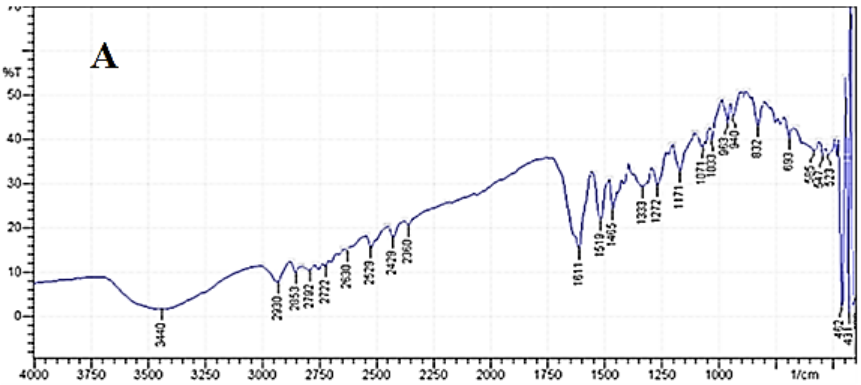

a)

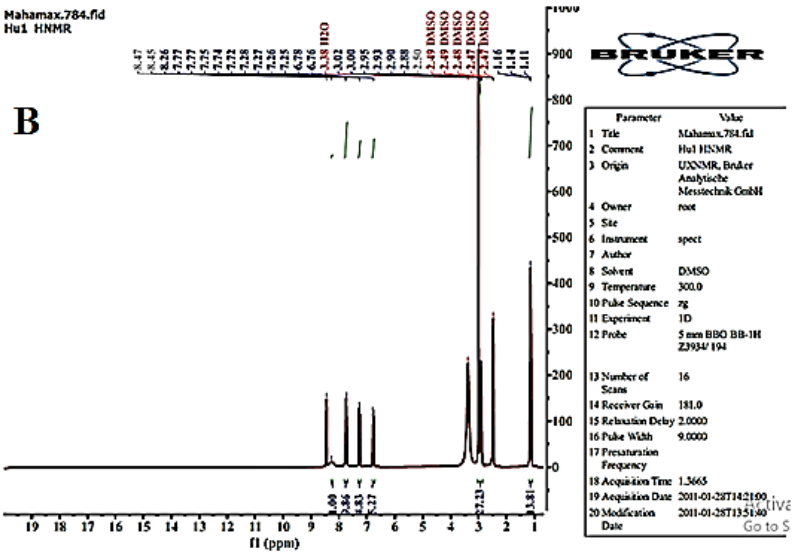

Figure 2. Diagnosis of AOMI (a) FT-IR (b) ^{1}H NMR

3.2 Weight loss results

According to Eq. 1 [17], the difference of a mass (ΔW) is divided by the surface area of the mild steel sample (A) and time of the test (t). Furthermore, the corrosion rate in the inhibited acidic solution (CR^{in}) and uninhibited one (CR^{un}) (Eq. 2) can be used to evaluate the inhibitor's performance ($\%IE_w$) [18]. The outcomes are displayed in Table 1. It is clear that the corrosion rate increased with temperature and decreased with the inhibitor concentration. The development of a protective layer on the metal surface may be the cause of the corrosion rate decrease when AOMI is present.

$$CR = \frac{\Delta W}{A \times t} \quad (1)$$

$$\%IE_w = \frac{CR^{un} - CR^{in}}{CR^{un}} \times 100 \quad (2)$$

Table 1: Corrosion rate outcomes from the mass loss tests as a function of temperature and AOMI concentrations

Test no.	C_{AOMI} (ppm)	T (°C)	C.R. (g.m^{-2}.day^{-1})	Surface coverage (Θ)	%IE$_w$
1	Blank	30	131.23	-	-
2		40	315.45	-	-
3		50	627.43	-	-
4		60	1614.34	-	-
5	20	30	63.32	0.51	50.12
6	40		55.73	0.57	57.55
7	60		39.42	0.69	69.97
8	80		39.52	0.72	72.18
9	20	40	91.32	0.71	71.05
10	40		59.45	0.81	81.15
11	60		53.31	0.83	83.11
12	80		46.71	0.85	85.19
13	20	50	161.31	0.74	74.29
14	40		102.21	0.84	83.70
15	60		82.41	0.86	86.86
16	80		78.21	0.87	87.53
17	20	60	363.21	0.77	77.50
18	40		258.21	0.84	84.00
19	60		209.23	0.87	87.01
20	80		175.68	0.90	90.00

3.3 Influence of temperature and activation parameters

Temperature is a significant element in the corrosion process because it determines the rate at which chemical reactions occur. As shown in Figure 3, the influence of temperature in the uninhibited and inhibited 1M HCl was illustrated in term of Arrhenius equation (Fig. 3A) and transition-state equation (Fig. 3B) [19]. Table 2 presents the parameters derived from Figure 3.

$$CR = A \exp\left(\frac{-E_a}{RT}\right) \quad (3)$$

$$CR = \frac{RT}{Nh} \exp\left(\frac{\Delta S_a}{R}\right) \exp\left(\frac{-\Delta H_a}{RT}\right) \quad (4)$$

In these equations, A, Ea, R, T, h, N, ΔH_a and, ΔS_a represent the pre-exponential factor, activation energy, gas constant, absolute temperature, Planck's constant, Avogadro's number, activation enthalpy, and activation entropy, respectively. As can be observed, adding AOMI causes the activation energy to drop in comparison to the control. Furthermore, the endothermic nature of the dissolving process is represented in the positive activation enthalpy. The entropy of activation in the presence of AOMI is large and negative, showing that disorder decays during the adsorption on the metal surface [20]. Furthermore, in the inhibited solutions compared to the uninhibited solution, ΔS_a values are more positive. This result is explained by the chemical substitution mechanism that occurs during inhibitor adsorption on the steel surface [21].

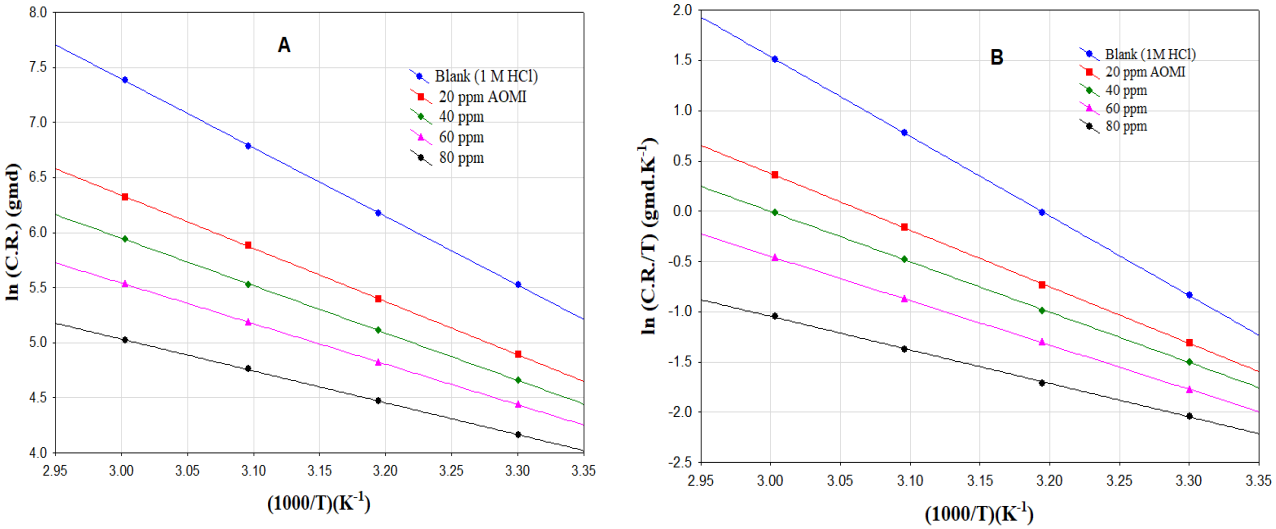

a) b)

Figure 3. A-Arrhenius plots. **B**- Transition state plots.

Table 2: Parameters of activation for the corrosion of mild steel in 1M HCl in the absence and presence of AOMI

C_{AOMI} (ppm)	A (gmd)	E_a (kJ/mol)	ΔH_a (kJ/mol)	ΔS_a (J/mol.K)
Blank	2.2×10^3	51.88	65.78	-181.65
20	7.2×10^2	40.15	46.78	-192.24
40	4.7×10^2	35.78	41.60	-195.67
60	3.0×10^2	30.62	36.66	-199.51
80	1.8×10^2	24.05	27.69	-205.02

3.4 Influence of inhibitor concentration and adsorption parameters

The adsorption process of inhibitor is very important to understand the mechanism of the inhibition. Several adsorption models are fitted to surface coverage data (θ=%IE_W/100), which obtained from the weight loss test. Freundlich, Flory-Huggins, EI-Awady, and Langmuir models were used to check the best model [22–25]. According to the graphical representation (Figure 4) and correlation coefficient (R^2), the best fit was according to the Langmuir adsorption isotherm (Eq. 5).

$$\frac{C}{\theta} = \frac{1}{K_{ads}} + C \quad (5)$$

K_{ads} is the equilibrium constant (adsorption constant). Furthermore, ΔG_{ads}, ΔH_{ads}, and ΔS_{ads} for the adsorption process were computed using Eq. 6, Eq.7 (Fig. 5A), and Eq. 8 (Figure 5B), respectively [26].

$$K_{ads} = \frac{1}{55.5} \exp\left(\frac{-\Delta G_{ads}}{RT}\right) \quad (6)$$

$$\ln K_{ads} = -\frac{\Delta H_{ads}}{RT} + constant \quad (7)$$

$$\Delta G_{ads} = \Delta H_{ads} - T\Delta S_{ads} \quad (8)$$

All data was collected in Table 3. The best fit was according to the Langmuir adsorption isotherm. Temperature-dependent increases in K_{ads} values indicate improved adsorption at high temperatures. The range of Gibbs free energy (ΔG_{ads}) is between -40 and -20 kJ/mol, suggesting that AOMI spontaneously adsorbed through both chemical and physical adsorption on the mild steel surface [27]. The values of the entropy and enthalpy of adsorption were 0.121 J. $mol^{-1}.K^{-1}$ and 35.272 kJ mol^{-1}, respectively. The adsorption of AOMI is an exothermic reaction, as indicated by the negative sign of the adsorption enthalpy. The entropy of adsorption was negative and it agreed with some literature values [28]. Thermodynamic principles also dictate that since adsorption was an exothermic process, there had to be a decrease in entropy.

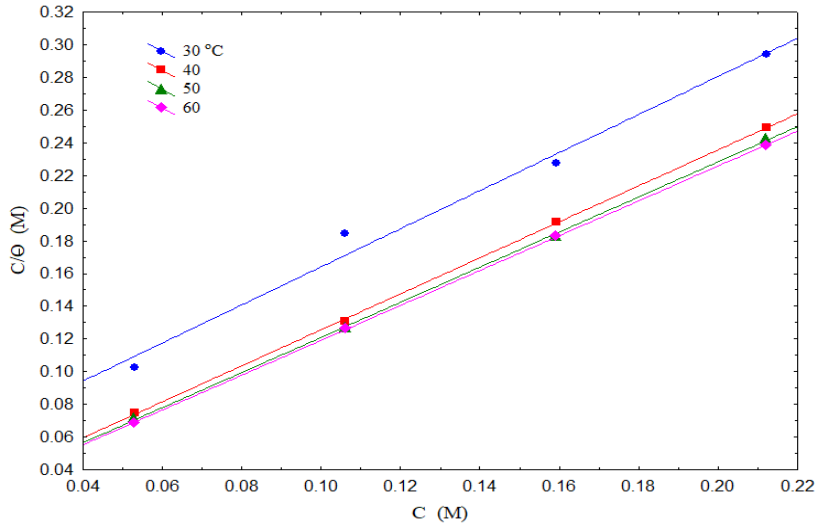

Figure 4. Langmuir adsorption isotherm.

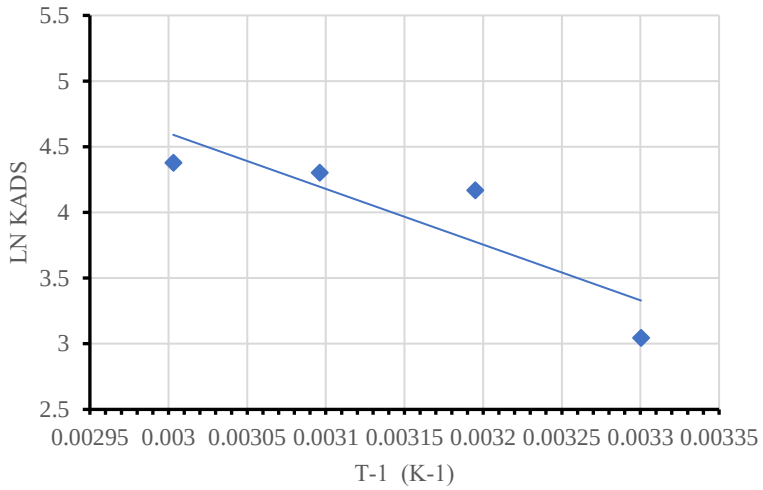

a)

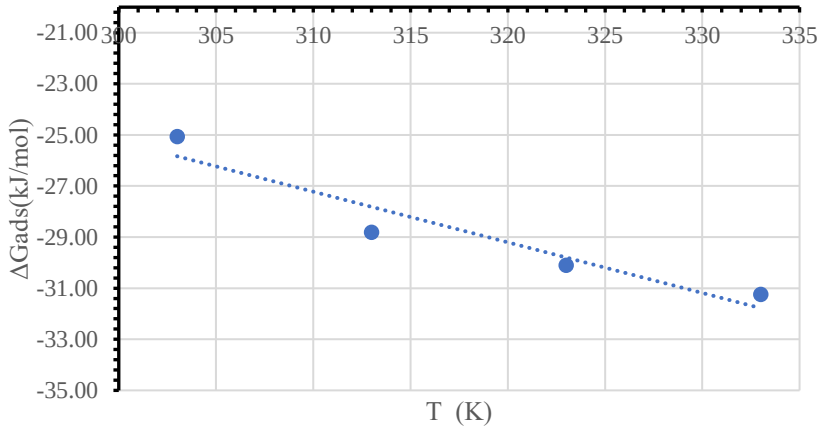

b)

Figure 5. (A) The VanHoff plot and (B) Heat of adsorption.

Table 3: Parameters of adsorption of AOMI on mild steel surface in 1M HCl

T (K)	K_{ads} (M^{-1})	R^2	ΔG_{ads} ($kJ.mol^{-1}$)	ΔH_{ads} ($kJ.mol^{-1}$)	ΔS_{ads} ($kJ.mol^{-1}.K^{-1}$)
303	20.98	0.9935	-25.07	35.272	0.121
313	64.54	0.9999	-28.82		
323	73.89	0.9999	-30.10		
333	79.74	0.9999	-31.24		

3.5 Electrochemical results

The OCP variation with time is displayed in Fig. 6A. After around 60 minutes, the steady-state potential was attained. A Tafel curve (Fig. 6B) can be used to illustrate the relationship between the over potential and the logarithmic current density. The extrapolation method can then be used to calculate the Tafel slopes (β_a and β_c), corrosion potential (E_{corr}), and corrosion current density (I_{corr}) [29, 30]. Furthermore, Eq. 9 was utilized to compute the inhibitory efficiency (%IE_p) of the AOMI. The corrosion current densities (i_{corr}) in the presence and

absence of AOMI are denoted by the variables i_{corr}^{un} and i_{corr}^{in} in Eq. 9. Table 4 contains all of the electrochemical characteristics gathered from the Tafel and OCP plots.

$$\%IE_p = \frac{i_{corr}^{un} - i_{corr}^{in}}{i_{corr}^{un}} \times 100 \quad (9)$$

The addition of AOMI only slightly altered the Tafle anodic and cathodic slopes [31]. Corrosion current density degreased in the presence of 80 ppm of AOMI, accounting for 89.12% of inhibitory efficiency. $\%IE_p$ was in good agreement with weight loss inhibition efficiency ($\%IE_w$ equal to 90.00% at 80 ppm and 60 ^oC). The E_{corr} value is used to determine the type of corrosion inhibitor. If the E_{corr} value is larger than 85 mV relative to the blank solution, the inhibitor operates as either a cathodic or anodic type, whereas a value less than 85 mV acts as both. In the current investigation, the difference between E_{corr} of the inhibited and uninhibited solution is 45.7 mV (Table 4), indicating a mixed-type inhibitor [32-36].

Figure 6C and D are the Nyquist and Bode graphs. Furthermore, Eq. 10 was utilized to compute the inhibition efficiency ($\%IE_E$) of the AOMI. The resistance of the charge transfer in the presence and absence of AOMI are represented by R_{ct}^{un} and R_{ct}^{in}, respectively, in Eq. 10. Table 5 shows all electrochemical parameters.

$$\%IE_E = \frac{R_{ct}^{in} - R_{ct}^{un}}{R_{ct}^{in}} \times 100 \quad (10)$$

Evidently, the inclusion of AOMI causes the R_{ct} to rise from 12.09 to 106.05 $\Omega.cm^2$. A protective coating has formed due to adsorption od AOMI on the metal surface, as indicated by the C_{dl} decreasing.

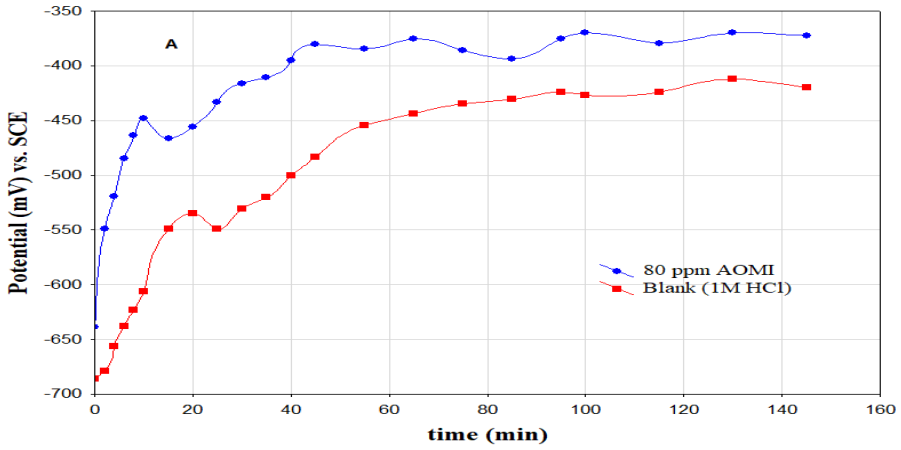

a)

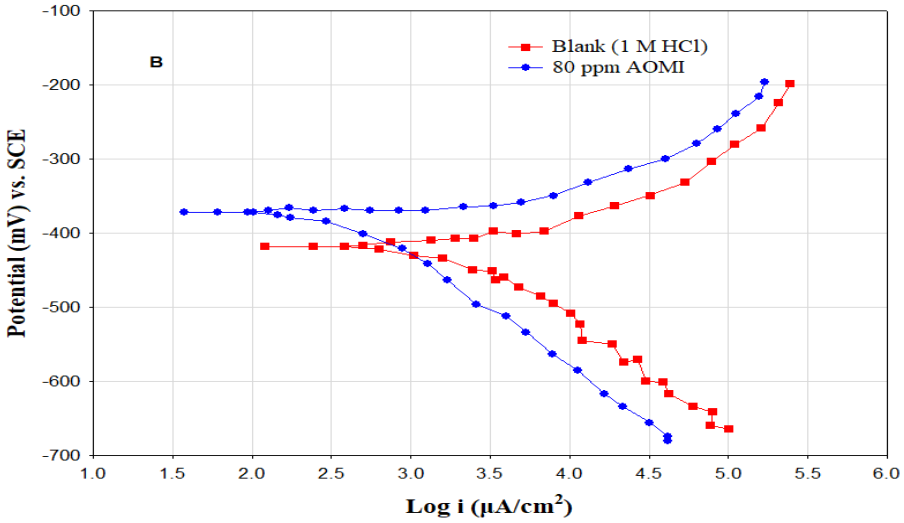

b)

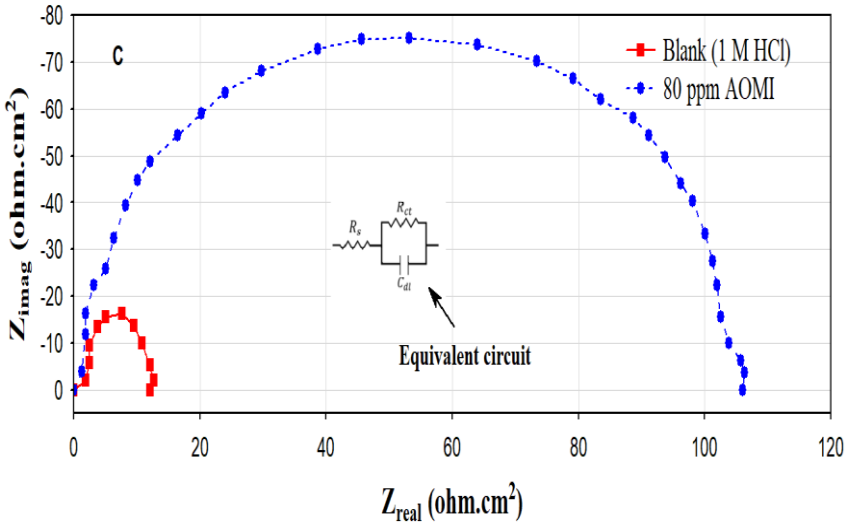

c)

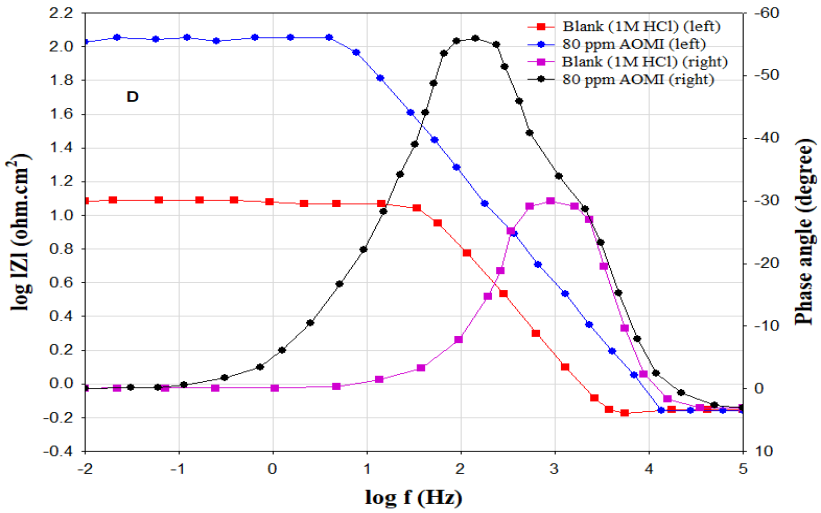

d)

Figure 6. Electrochemical representations **(a**) OCP, **(b)** PDP, **(c)** Nyquist **(d)** Bode & phase angle plots of experimental data. (All for mild steel in 1 M HCl without and with 80 ppm AOMI at 60 °C).

Table 4: PDP parameters.

Inhibitor	OCP (mV) SCE	E_{corr} (mV) SCE	I_{corr} (µA/cm^2)	βc (mV/dec)	βa (mV/dec)	%IEp
Blank	-419.5	-417.6	6457.4	-110	71	–
AOMI	-371.59	-371.82	702.72	-228	68	89.12

Table 5: EIS parameters.

Inhibitor	R_s (Ω.cm^2)	R_{ct} (Ω.cm^2)	C_{dl} (µF.cm^{-2})	%IE_E
Blank	0.71	12.1	101	–
AOMI	0.696	106.05	49.57	88.60

3.6 Surface morphological results

Figures 7A, B, and C show SEM graphs. In Figure 7A (samples before test), the surface appeared undamaged. In Figure 7B (1M HCl for 3h at 60 ^{o}C), severe corrosion was observed. In Figure 7C (1M HCl+80 ppm AOMI for 3h at 60 ^{o}C) an improvement in surface was observed.

Figure 8 showed AFM images under same conditions of SEM. Table 6 lists the AFM parameters. These parameters were arithmetic mean height (Sa), maximum height (S_z), and root mean square height (S_q). S_q, S_z, and S_a measured 11.96, 54.61, and 9.95 nm, for cas A, B, and C, respectively, in the polished sample. In the blank answer, the numbers increased by 68.5, 86.1, and 65.6%, respectively. However, due of the inhibitor molecules' adsorption on the metal surface, the surface values.

Figure 9 shows the XRD spectra at the same conditions of SEM and AFM. In the case of a bare or polished mild steel surface, the diffraction peaks at about 44° and 65° were attributed to iron peaks. Moreover, the peak around 30° was observed in the case of mild steel immersion in blank solution, which is related to the formation of the oxide films on the metal surface [37]. On the other hand, no diffraction peaks were mentioned for the mild steel immersion in the inhibited solution, and the oxide layer was suppressed. These results highlight how the AOMI inhibitor forms a protective coating on the metal surface, so minimizing the corrosive solution attack.

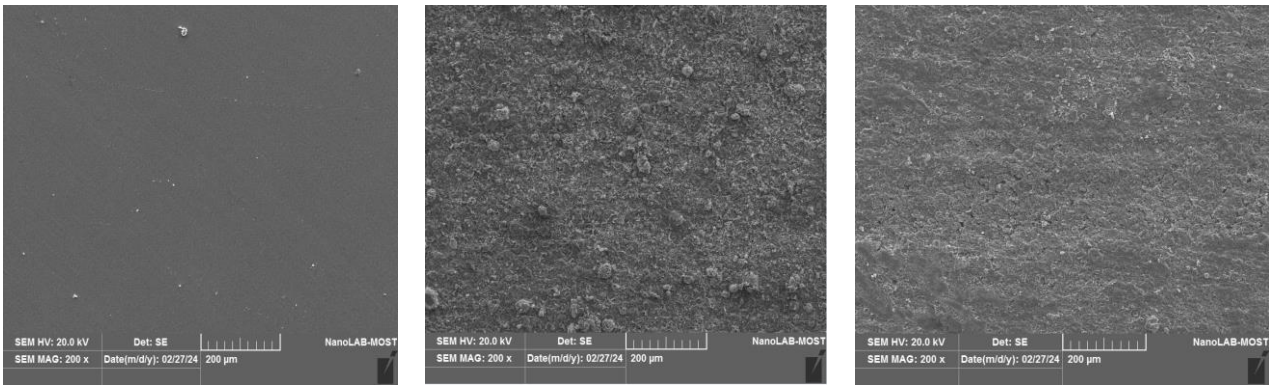

A B C

Figure 7. The SEM images **(A)** Polished before test **(B)** 1 M HCl alone **(C)** 1 M HCl + 80ppm AOMI at 60°C.

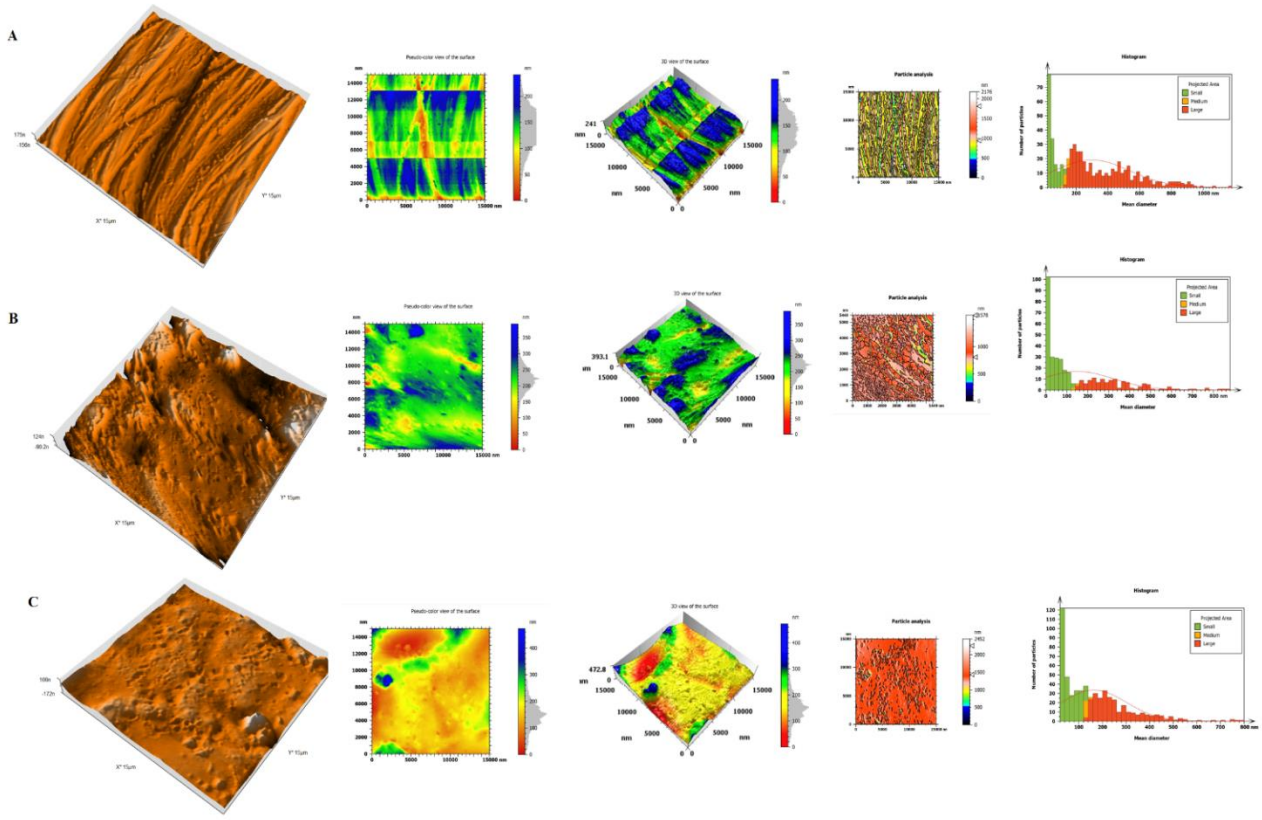

Figure 8. AFM images. A) Polished samples. B) After immersion for 3 h in blank 1M HCl at 60 °C. c) After 3h immersion in the presence of 80 ppm AOMI at 60 °C.

Table 6: Parameters of AFM for mild steel surface at different conditions

Case	S_q (nm)	S_z (nm)	S_a (nm)
Before test	11.96	54.61	9.95
1M HCl	38.01	393.1	28.91
80 ppm AOMI+1M HCl	25.11	145.2	19.97

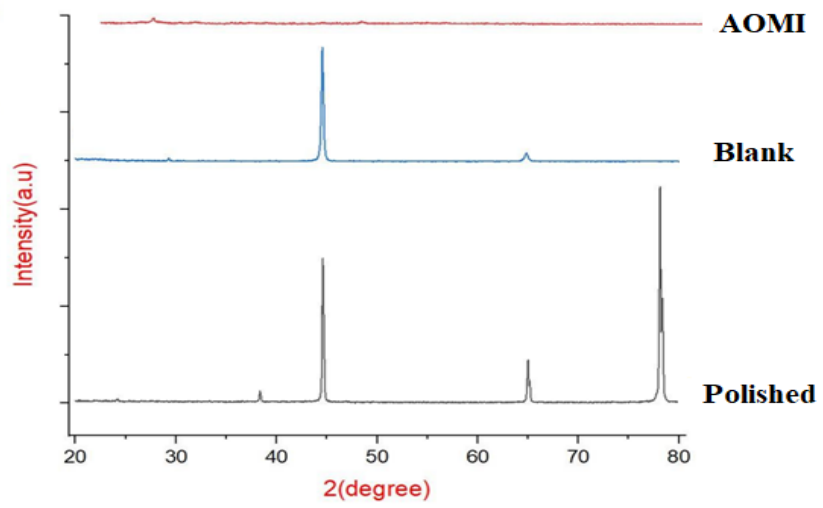

Figure 9. XRD Surface images after 3h corrosion exposure of mild steel (A283/C) (A) in 1 M HCl solution at 60 °C, 80 ppm for a polished sample before corrosion run, without inhibitor, and with AOMI

3.7 Uv-vis results

As illustrated in Figure 10, UV-Vis spectra were obtained both before and after three hours of dipping. The range of the absorption unit in the AOMI absorption spectrum prior to immersion is 3.55 to 4.54 units. However, after three hours of immersion in 1M HCl, the spectrum of absorption was lower. This can be attributed to the interaction between the mild steel surface and AOMI [38].

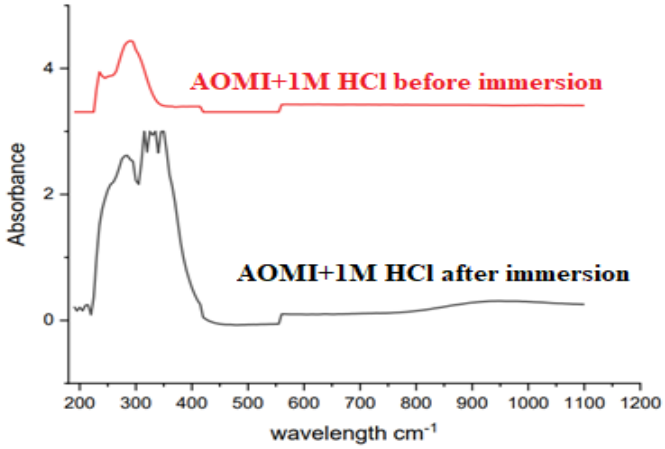

Figure 10. UV-spectra of AOMI + 1M HCl.

3.8 Quantum chemical and theoretical results

ArgusLab website software was used during calculations. Geometry and energies were optimized based on Austin Model 1 (AM1), 200 maximum iterations, and 10^{-10} kcal/mol convergence. Figure 11 displays the distribution of the optimized structure, density maps, HOMO, and LUMO. The nearly uniform distribution implies that the molecule might readily adhere to the surface of mild steel.

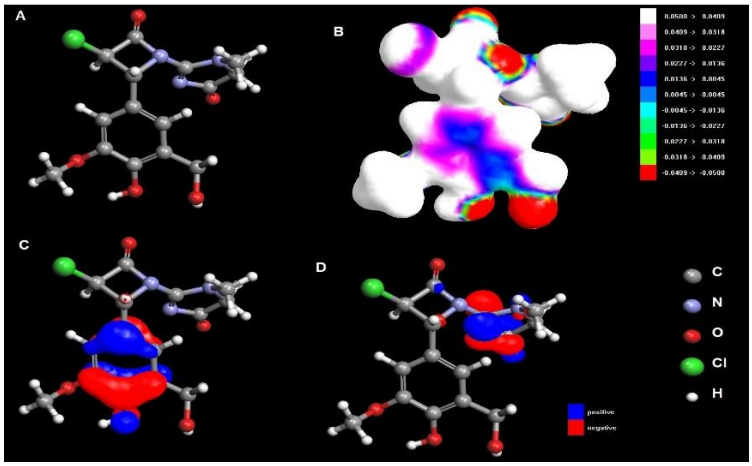

Figure 11. Quantum chemical illustrations of AOMI. (A) Optimized molecular structure, (B) Density map molecular distribution, (C) HOMO molecular distribution, and (D) LUMO molecular distribution.

A number of quantum chemical data were determined and compiled in Table 7, including the heat of formation (ΔH_f), dipole moment (μ), proportion of electron transfer (ΔN), energy gap (E_{gap}), lowest unoccupied molecular orbital energy (E_{LUMO}), and the highest occupied molecular orbital energy (E_{HOMO}). The E_{LUMO} and E_{HOMO} values indicate how well a molecule can take in and give away electrons. Put differently, an inhibitor that has a higher E_{HOMO} has a higher probability of transferring electrons to the appropriate d-orbital of the metal. On the other hand, if an inhibitor has a lower E_{LUMO}, it means that during the back-donation process, The molecule is more probable to allow electrons from the metal orbitals. The relationship between the energy of the border molecular orbital and corrosion inhibition efficacy may be better understood using the energy gap [39]. The correlation between the E_{gap} value and the molecular capacity to halt corrosion is inverse. The denser adsorption and the greater the corrosion inhibition effect, the smaller the energy gap [40-44]. For AOMI, the gap value is 9.012 eV.

Table 7: AOMI quantum chemical parameters

E_{HOMO} (eV)	E_{LUMO} (eV)	E_{gap} (eV)
-9.611	-0.598	9.012

3.9 Mechanism of inhibition and comparison study

The electrochemical investigations demonstrated that AOMI acted as a mixed-type inhibitor. It had an effect on both cathodic and anodic reactions. Furthermore, it was determined that the inhibitory process was caused by the formation of a protective layer on the surface of mild steel. AOMI molecules adsorb onto mild steel surfaces, preventing corrosive species from making contact with the metal. In acidic conditions, the positively charged mild steel surface interacts electrostatically with cationic inhibitor molecules. Furthermore, chloride ions from HCl acid aid the adsorption process by producing a Fe-Cl- layer (physical adsorption) [45]. In addition to electrostatic adsorption, the inhibitors probably establish strong covalent bonds (chemical adsorption) with the mild steel surface. Quantum chemical theoretical calculations confirm this proposed mechanism. The carbonyl groups (C=O), nitrogen, and oxygen atoms appear to have a particularly strong bonding affinity [46]. Figure 12 explains a simplified illustration of the proposed inhibition mechanism of AOMI molecules on the mild steel surface in HCl acid.

Imidazole derivatives were widely synthesized and used as corrosion inhibitors [47, 48]. Many studies in the literature demonstrate great performance for imidazole derivatives with a high percentage of the inhibitory efficiencies (around 95%) [49-51]. Therefore, AOMI shows a significant protection efficiency as compared with others imidazole derivatives [52, 53].

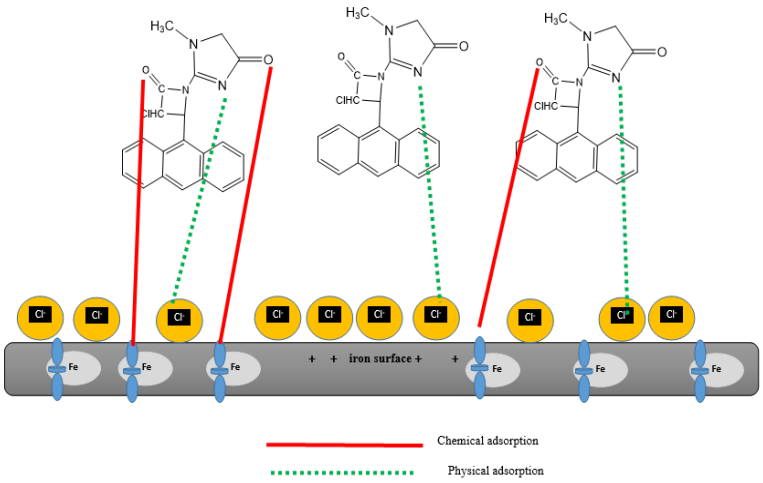

Figure 12. The proposed inhibition mechanism of AOMI molecules on the mild steel surface in HCl acid

4. Conclusion

Over the implementation of experimental and theoretical techniques, the following conclusions were obtained:

1. It was found that the corrosion rate of the mild steel in hydrochloric acid increased with temperature and decreased with inhibitor concentration.
2. Weight loss data showed that AOMI can successfully adsorb at the metal/solution interface, thus decreasing the mild steel corrosion caused by HCl. The adsorption process was according to the Langmuir monolayer adsorption model.
3. Maximum corrosion inhibition efficiency was 90%at 80 ppm and 60 ^{o}C.
4. The electrochemical measurement results show that AOMI is a significant mixed-type corrosion inhibitor in a mild steel and hydrochloric acid system.
5. The quantum chemical computations served as an effective theoretical instrument to validate the experimental results.

References

[1] A. A. Mansour, C. Hejjaj, F. Z. Thari, K. Karrouchi, L. Bazzi, K. Bougrin, R. Salghi, et al., "Interfacial phenomena and surface protection of N80-carbon steel in acidic environments using thiazolidinediones: An experimental and computational analysis," *Colloids and Surfaces A: Physicochemical and Engineering Aspects*, vol. 677, Nov 2023

[2] A. Singh, K. R. Ansari, M. A. Quraishi, H. Lgaz, Y. Lin, et al., "Synthesis and investigation of pyran derivatives as acidizing corrosion inhibitors for N80 steel in hydrochloric acid: Theoretical and experimental approaches," *Journal of Alloys and Compounds*, vol. 762, pp. 347-362, Sep 2018.

[3] A. Ghaidan, A. J. Jomah "Enhancing Mechanical Properties of Low Alloy Steel through Novel Molten Bi-Ga Austempering,"*Diyala Journal of Engineering Sciences*, vol. 17, pp. 173-181, June 2024.

[4] A. Rahimi, M. Abdouss, A. Farhadian, L. Guo, S. Kaya, J. Neshati, et al., "Enhancement corrosion resistance of mild steel in 15% HCl solution by a novel bio-based polyurethane for oil well acidizing," *Journal of Industrial and Engineering Chemistry*, vol. 113, pp. 332-347, Sep 2022.

[5] R. K. Mehta, M. Yadav, I. B. Obot, et al., "Electrochemical and computational investigation of adsorption and corrosion inhibition behaviour of 2-aminobenzohydrazide derivatives at mild steel surface in 15% HCl," *Materials Chemistry and Physics*, vol. 290, Oct 2022.

[6] Z. I. Jasim, K. H. Rashid, K. F. AL-Azawi, A. A. Khadom, et al., "Optimization of the corrosion inhibition performance of novel oxadiazole thione-based Schiff base for mild steel in HCl media using Doehlert experimental design," *Inorganic Chemistry Communications*, vol. 160, 2024.

[7] Z. I. Jasim, K. H. Rashid, A. A. Khadom, et al., "Corrosion and corrosion control of the steel in acidizing oil wells processes: An overview of organic inhibitors," *Russian Journal of Applied Chemistry*, vol. 97, no. 1, pp. 1-19, Apr 2024.

[8] K. F. Al-azawi, Z. W. Ahmed, E. H. Ali, A. A. Khadom, H. H. Abrahim, K. H. Rashid, et al., "Synthesis and characterization of (E)-4-(((4-(5-mercapto-1, 3, 4-oxadiazol-2-yl) phenyl) amino)

methyl)-2-methoxyphenol as a novel corrosion inhibitor for mild-steel in acidic medium," *Results in Chemistry*, vol. 5, May 2023.

[9] Z. I. Jasim, K. H. Rashid, K. F. AL-Azawi, A. A. Khadom, et al., "Synthesis of schiff-based derivative as a novel corrosion inhibitor for mild steel in 1M HCl solution: optimization, experimental, and theoretical investigations," *Journal of Bio-and Tribo-Corrosion*, vol. 9, no. 54, Jun 2023

[10] W.F. Hameed, K. H. Rashid, A.A. Khadom, et al., "Investigation of tetraazaadamantane as corrosion inhibitor for mild steel in oilfield produced water under sweet corrosive environment, " *Journal of Bio-and Tribo-Corrosion*, vol. 8, no. 27, pp. 1-19. Dec 2022.

[11] K. T. Loganathan, V. S. Thimmakondu, S. Nagarajan, R. Natarajan, et al., "Corrosion inhibitive evaluation and DFT studies of 2-(Furan-2-yl)-4, 5-diphenyl-1H-imidazole on mild steel at 1.0 M HCl, " *Journal of the Indian Chemical Society*, vol. 98, no. 19, Aug 2021.

[12] G. Senthilkumar, C. Umarani, A. Ramachandran, et al., "Investigation on corrosion inhibition effect of N-[4-(1, 3-benzo [d] thiazol-2-ylcarbamoyl) phenyl] quinoline-6-carboxamide as a novel organic inhibitor on mild steel in 1N HCl at different temperatures: experimental and theoretical study," *Journal of the Indian Chemical Society*, vol. 98, no. 6, Jun 2021.

[13] H.S. Hassan, K.H. Rashid, K.F. AL-Azawi, A.A. Khadom, et al., "A combined experimental and theoretical study into the effect of new heterocyclic compound containing β-lactam ring as corrosion inhibitor for mild steel in hydrochloric acid, " *Results in Surfaces and Interfaces*, vol. 17, Oct 2024.

[14] C. Verma, L. O. Olasunkanmi, E. E. Ebenso, M. A. Quraishi, et al., "Substituents effect on corrosion inhibition performance of organic compounds in aggressive ionic solutions: a review," *Journal of Molecular Liquids*, vol. 251, pp. 100-118. Feb 2018.

[15] H. Gökce, F. Şen, Y. Sert, B. F. Abdel-Wahab, B. M. Kariuki, G. A. El-Hiti, et al., "Quantum computational investigation of (E)-1-(4-methoxyphenyl)-5-methyl-N′-(3-phenoxybenzylidene)-1 H-1, 2, 3-triazole-4-carbohydrazide," *Molecules*, vol. 27, no. 2193, pp. 1-22, Mar 2022.

[16] P. Koparır, R. Omer, M. Karatepe, L. Ahmed, et al., "Synthesis, Characterization, and theoretical inhibitor study for (1E, 1'E)-2, 2'-thiobis (1-(3-mesityl-3-methylcyclobutyl) ethan-1-one) dioxime, " *El-Cezerî Journal of Science and Engineering*, vol. 8, no. 3, pp. 1495-1510, Jul 2021.

[17] M. E. H. N. Tehrani, P. Ghahremani, M. Ramezanzadeh, G. Bahlakeh, B. Ramezanzadeh, et al., "Theoretical and experimental assessment of a green corrosion inhibitor extracted from Malva sylvestris," *Journal of Environmental Chemical Engineering*, vol. 9, no. 3, Feb 2021.

[18] F. Wedian, M. A. Al-Qudah, G. M. Al-Mazaideh, et al., "Corrosion inhibition of copper by Capparis spinosa L. extract in strong acidic medium: experimental and density functional theory, " *International Journal of Electrochemical Science*, vol. 12, no. 6, pp. 4664-4676, May 2017.

[19] O. I. El Mouden, A. Anejjar, R. Salghi, S. Jodeh, O. Hamed, I. Warad, R. S. Dassanayake, et al., "Inhibitive Action of Capparis Spinosa Extract on the Corrosion of Carbon Steel in an Aqueous Medium of Hydrochloric Acid," *Journal of Mineral Metal and Material Engineering*, vol. 1, pp. 1-7, Aug 2015.

[20] J. Lazrak, E. Ech-Chihbi, B. El Ibrahimi, F. El Hajjaji, Z. Rais, M. Tachihante, M. Taleb, et al., "Detailed DFT/MD simulation, surface analysis and electrochemical computer explorations of aldehyde derivatives for mild steel in 1.0 M HCl," *Colloids and Surfaces A: Physicochemical and Engineering Aspects*, vol. 632, Jan 2022.

[21] Y. Fernine, E. Ech-Chihbi, N. Arrousse, F. El Hajjaji, F. Bousraf, M. E. Touhami, M. Taleb, et al., "Ocimum basilicium seeds extract as an environmentally friendly antioxidant and corrosion inhibitor for aluminium alloy 2024-T3 corrosion in 3 wt% NaCl medium," *Colloids and Surfaces A: Physicochemical and Engineering Aspects*, vol. 627, no. 20, Oct 2021.

[22] A. Jmiai, B. El Ibrahimi, A. Tara, S. El Issami, O. Jbara, L. Bazzi, et al., "Alginate biopolymer as green corrosion inhibitor for copper in 1 M hydrochloric acid: experimental and theoretical approaches, " *Journal of Molecular Structure*, vol. 1157, pp. 408-417, Apr 2018.

[23] X. Xu, J. Qu, H. Huang, et al., "Synthesis of a dibenzimidazole compound and its corrosion inhibition behavior on AZ91D Mg alloy in 3.5 wt.% NaCl solution," *Journal of Molecular Structure*, vol. 1291, Nov 2023.

[24] A. R. Shahmoradi, N. Talebibahmanbigloo, C. Nickhil, R. Nisha, A. A. Javidparvar, P. Ghahremani, B. Ramezanzadeh, et al., "Molecular-MD/atomic-DFT theoretical and experimental studies on the quince seed extract corrosion inhibition performance on the acidic-solution attack of mild-steel," *Journal of Molecular Liquids*, vol. 346, Jan 2022.

[25] S. Geng, J. Hu, J. Yu, C. Zhang, H. Wang, X. Zhong, "Rosin imidazoline as an eco-friendly corrosion inhibitor for the carbon steel in CO_2-containing solution and its synergistic effect with thiourea," *Journal of Molecular Structure*, vol. 1250, Feb 2022.

[26] N. Benzbiria, A. Thoume, S. Echihi, M. E. Belghiti, A. Elmakssoudi, A. Zarrouk, M. Zertoubi, et al., "Coupling of experimental and theoretical studies to apprehend the action of benzodiazepine derivative as a corrosion inhibitor of carbon steel in 1M HCl, " *Journal of Molecular Structure*, vol. 1281, Feb 2023.

[27] N. N. Hau, D. Q. Huong, "Effect of aromatic rings on mild steel corrosion inhibition ability of nitrogen heteroatom-containing compounds: Experimental and theoretical investigation, " *Journal of Molecular Structure*, vol. 1277, Apr 2023.

[28] N. O. Obi-Egbedi, I. B. Obot, "Inhibitive properties, thermodynamic and quantum chemical studies of alloxazine on mild steel corrosion in H_2SO_4, " *Corrosion science*, vol. 53, pp. 263-275, Jan 2011.

[29] B. E. D. M. El-Gendy, S. T. Atwa, A. A. Ahmed, A. Y. El-Etre, et al., "Synthesis and characterization of carbon steel corrosion inhibitors based on 4, 5, 6, 7-tetrahydrobenzo [b] thiophene Scaffold, " *Protection of Metals and Physical Chemistry of Surfaces*, vol. 55, pp. 179-186, May 2019.

[30] L. Chen, D. Lu, Y. Zhang, et al., "Organic compounds as corrosion inhibitors for carbon steel in HCl solution: A comprehensive review, " *Materials*, vol. 15, no. 6, Mar 2022.

[31] U. J. Timothy, U. Mamudu, M. M. Solomon, P. S. Umoren, I. O. Igwe, P. I. Anyanwu, S. A. Umoren, et al., "In-situ biosynthesized plant exudate gums-silver nanocomposites as corrosion inhibitors for mild steel in hydrochloric acid medium, " *International Journal of Biological Macromolecules*, vol. 269, Jun 2024.

[32] K.H. Rashid, A.A. Khadom, S.H. Abbas, K. F. Al-azawi, H. B. Mahood, et al., "Optimization studies of expired mouthwash drugs on the corrosion of aluminium 7475 in 1M hydrochloric acid: Gravimetrical, electrochemical, morphological and theoretical investigations, " *Results in Surfaces and Interfaces*, vol.13, 2023.

[33] D. K. Verma, F. Khan, "Corrosion inhibition of mild steel in hydrochloric acid using extract of glycine max leaves," *Research on Chemical Intermediates*, vol. 42, pp. 3489-3506, 2016.

[34] K.H. Rashid, A.A. Khadom, H.B. Mahood, A. N. Campbell, et al., "The effect of mass transfer on corrosion in oilfield production processes by wastewater enriched with CO_2: computer-aided modelling and experimental verification," *Case Studies in Chemical and Environmental Engineering*, vol. 2, Jul 2020.

[35] M. Salman, K. R. Ansari, J. Haque, V. Srivastava, M. A. Quraishi, M. A. Mazumder, et al., "Ultrasound-assisted synthesis of substituted triazines and their corrosion inhibition behavior on N80 steel/acid interface," *Journal of Heterocyclic Chemistry*, vol. 57, pp. 2157-2172, May 2020.

[36] S.A. Hussein, A.A. Khadom, A.A.H. Kadhum, H.B. Mahood, K.H. Rashid, et al., "Mass transfer influence on the corrosion inhibition of N80 steel in 1M H_2SO_4 by green corrosion inhibitor using MATLAB," *International Journal of Electrochemical Science*, vol. 19, Aug 2024.

[37] R. Hsissou, F. Benhiba, M. Khudhair, M. Berradi, A. Mahsoune, H. Oudda, A. Zarrouk, et al., "Investigation and comparative study of the quantum molecular descriptors derived from the theoretical modeling and Monte Carlo simulation of two new macromolecular polyepoxide architectures TGEEBA and HGEMDA," *Journal of King Saud University-Science*, vol. 32, pp. 667-676, Jan 2020.

[38] M. Gopiraman, N. Selvakumaran, D. Kesavan, R. Karvembu, et al., "Adsorption and corrosion inhibition behaviour of N-(phenylcarbamothioyl) benzamide on mild steel in acidic medium, " *Progress in Organic Coatings*, vol. 73, pp. 104-111, Jan 2012.

[39] E. A. Erazua, B. B. Adeleke, "A Computational Study of Quinoline Derivatives as Corrosion Inhibitors for Mild Steel in Acidic Medium, " *Journal of Applied Sciences and Environmental Management*, vol. 23, no.10, pp. 1819-1824, Nov 2019.

[40] S. K. Saha, P. Ghosh, A. Hens, N. C. Murmu, P. Banerjee, et al., "Density functional theory and molecular dynamics simulation study on corrosion inhibition performance of mild steel by mercapto-quinoline Schiff base corrosion inhibitor, " *Physica E: Low-dimensional systems and nanostructures*, vol. 66, pp. 332-341, Feb 2015.

[41] A. Singh, K. R. Ansari, J. Haque, P. Dohare, H. Lgaz, R. Salghi, M. A. Quraishi, et al., "Effect of electron donating functional groups on corrosion inhibition of mild steel in hydrochloric acid: Experimental and quantum chemical study, " *Journal of the Taiwan Institute of Chemical Engineers*, vol. 82, pp. 233-251, Jan 2018.

[42] A. S. Fouda, H. M. Abdel-Wahed, M. F. Atia, A. El-Hossiany, et al., "Novel porphyrin derivatives as corrosion inhibitors for stainless steel 304 in acidic environment: synthesis, electrochemical and quantum calculation studies, " *Scientific Reports*, vol. 13, Oct 2023.

[43] H. H. Rasul, D. M. Mamad, Y. H. Azeez, R. A. Omer, K. A. Omer, et al., "Theoretical investigation on corrosion inhibition efficiency of some amino acid compounds," *Computational and Theoretical Chemistry*, vol. 1225, Jul 2023.

[44] H. M. Elabbasy, A. Toghan, H. S. Gadow, et al., "Cysteine as an Eco-Friendly Anticorrosion Inhibitor for Mild Steel in Various Acidic Solutions: Electrochemical, Adsorption, Surface Analysis, and Quantum Chemical Calculations, " *ACS omega*, vol. 9, no. 11, pp. 13391-13411, Mar 2024.

[45] Z. Liu, F. Zhang, X. Li, D. Wang, et al., "Improved corrosion inhibition of calcium disodium EDTA for mild steel in chloride-contaminated concrete pore solution, " *Cement and Concrete Composites*, vol. 140, Apr 2023.

[46] B. Li, W. Wang, L. Chen, X. Zheng, M. Gong, J. Fan, G. Zhu, et al., "Corrosion inhibition effect of magnolia grandiflora leaves extract on mild steel in acid solution," *International Journal of Electrochemical Science*, vol. 18, Jul 2023.

[47] A. Tazouti, N. Errahmany, M. Rbaa, M. Galai, Z. Rouifi, R. Touir, S. Erkan, et al., "Effect of hydrocarbon chain length for acid corrosion inhibition of mild steel by three 8-(n-bromo-R-alkoxy) quinoline derivatives: experimental and theoretical investigations," *Journal of Molecular Structure*, vol. 1244, Nov 2021.

[48] K. Alaoui, M. Ouakki, A. S. Abousalem, H. Serrar, M. Galai, S. Derbali, Y. El Kacimi, et al., "Molecular dynamics, Monte-Carlo simulations and atomic force microscopy to study the interfacial adsorption behaviour of some triazepine carboxylate compounds as corrosion inhibitors in acid medium, " *Journal of Bio-and Tribo-Corrosion*, vol. 5, no. 1, 2019.

[49] H. M. Elabbasy, A. Toghan, H. S. Gadow, et al., "Cysteine as an Eco-Friendly Anticorrosion Inhibitor for Mild Steel in Various Acidic Solutions: Electrochemical, Adsorption, Surface Analysis, and Quantum Chemical Calculations, " *ACS omega*, vol. 9, no. 11, pp. 13391-13411, 2024.

[50] L. Zhang, Y. He, Y. Zhou, R. Yang, Q. Yang, D. Qing, Q. Niu, et al., "A novel imidazoline derivative as corrosion inhibitor for P110 carbon steel in hydrochloric acid environment," *Petroleum*, vol. 1, no. 3, pp. 237-243, Nov 2015.

[51] M. Galai, M. Rbaa, Y. E. Kacimi, M. Ouakki, N. Dkhirech, R. Touir, M. E. Touhami, et al., "Anti-corrosion properties of some triphenylimidazole substituted compounds in corrosion inhibition of carbon steel in 1.0 M hydrochloric acid solution", *Analytical and Bioanalytical Electrochemistry*, vol. 9, no. 1, pp. 80-101, Feb 2017.

[52] M. Rbaa, M. Galai, Y. El Kacimi, M. Ouakki, R. Touir, B. Lakhrissi, M. Ebn Touhami, et al., "Adsorption properties and inhibition of carbon steel corrosion in a hydrochloric solution by 2-(4, 5-diphenyl-4, 5-dihydro-1h-imidazol-2-yl)-5-methoxyphenol," *Electrochim. Acta*, vol. 35, no. 6, pp. 323-338, Apr 2017.

[53] M. Ouakki, M. Rbaa, M. Galai, B. Lakhrissi, E. H. Rifi, M. Cherkaoui, et al., "Experimental and quantum chemical investigation of imidazole derivatives as corrosion inhibitors on mild steel in 1.0 M hydrochloric acid," *Journal of Bio-and Tribo-Corrosion*, vol. 4, no. 35, pp. 1-14, May 2018.